Chemistry & Biology, Vol. 9, 813–819, July, 2002, ©2002 Elsevier Science Ltd. All rights reserved. PII S1074-5521(02)00166-7

Natural Supramolecular Building Blocks: Cysteine-Added Mutants of Cowpea Mosaic Virus

Qian Wang,[1] Tianwei Lin,[2] John E. Johnson,[2,3] and M.G. Finn[1,3]
[1]Department of Chemistry and
The Skaggs Institute for Chemical Biology
The Scripps Research Institute
[2]Department of Molecular Biology
The Scripps Research Institute
10550 North Torrey Pines Road
La Jolla, California 92037

Summary

Wild-type Cowpea mosaic virus (CPMV) displays no cysteine side chains on the exterior capsid surface and is therefore relatively unreactive with thiol-selective reagents. Four CPMV mutants bearing cysteine residues in one of two exterior positions of the asymmetric unit were created. The mutants were shown to aggregate by virtue of disulfide bond formation in the absence of added reducing agent, bind to metallic gold, and undergo selective reactions at the introduced thiol residues. Controlled aggregation by virtue of biotin-avidin interactions was demonstrated, as was the independent derivatization of reactive lysine and cysteine positions. The ability to introduce such reactivity into a system that can be readily prepared and isolated in gram quantities should open new doors to applications in biochemistry, materials science, and catalysis.

Introduction

In the accompanying paper we describe the chemical reactivity of wild-type Cowpea mosaic virus (CPMV) toward lysine-selective reagents. As we have briefly discussed elsewhere [1], the crystal structure of the wild-type structure displays no cysteine residues on its outside surface, and indeed reactions of the virus with such thiol-selective moieties as N-bromoacetamides and maleimides are slow and give alkylation of thiol residues located exclusively on the *interior* surface of the protein capsid. Here we show how the biological nature of the virus can be exploited to introduce designed chemical reactivity to the protein shell for nonbiological purposes.

Results and Discussion

Mutagenesis

Previous work designed to employ CPMV as a scaffold for the presentation of antigenic peptide sequences established that extra amino acids could be inserted into either of two solvent-exposed sites without compromising the ability of the resulting mutant virus to propagate in the host plant [2–5]. These sites, the βB-βC loop of the small subunit and the βE-βF loop of the large subunit, are shown in Figure 1. In order to convert the sluggish reactivity of wild-type CPMV to a thiol-rich exterior structure, we prepared the four mutant viruses shown in Figure 1B by using standard cloning techniques. The details of these procedures and certain aspects of the virus biology revealed by these studies will be described separately. However, it should be noted that the yield of each virus is 0.5–1.5 g per kg of infected leaves, and the altered sequences are genetically stable through multiple rounds of infection, harvesting, and reinoculation. Each of the virus mutants contains a cysteine residue inserted as part of an added small loop (**1**, **2**, **4**) or as a point mutation (**3**), and thus each particle contains 60 such insertions arrayed in icosahedral symmetry about the 30-nm-diameter capsid. Below, we focus on the chemistry of the resulting virus particles; in each case, the added residue proved to be chemically addressable.

Virus Aggregation

The unique chemistry of the cysteine mutants was immediately apparent upon their isolation. If no precautions are taken to maintain a reducing environment, each undergoes largely irreversible aggregation and precipitation in the first concentration step of the extraction procedure, presumably by the formation of a network of interparticle disulfide linkages. Virus **1** was an extreme case; it showed aggregation by transmission electron microscopy (TEM) during its purification from the leaves of the host plant and irreversible precipitation within one day at 4°C. The inserted peptide of **1** was also found to be subject to variable amounts of proteolytic cleavage either in the plant or during purification (Figure 2A, lanes 2 and 7), turning a "loop" into a dangling "strand" and probably facilitating aggregation. Such cleavage of inserted sequences is known [6, 7] and is the subject of current study in our laboratories. The other viruses described here exhibited no such cleavage. Remaining unchanged in solution for two days at concentrations less than 1 mg/ml, viruses **2–4** were much more resistant to aggregation than **1**. Their stability is presumably due to the lack of a protruding inserted loop at the more exposed βB-βC region for **2** (in contrast to **1**) and the generally more shielded environment of the βE-βF region for **3** and **4**. Reducing agents such as β-mercaptoethanol (BME) and dithiothreitol (DTT) at 10 mM concentration inhibited aggregation of all the cysteine mutants; 10 mM tris(2-carboxyethyl)phosphine (TCEP) provided long-term stabilization of **2–4** and did not inhibit covalent reactions with maleimides or related electrophiles.

Binding to Metallic Gold

To test the ability of the mutant viruses to bind to metallic gold surfaces, we incubated freshly prepared gold particles with an average diameter of 0.9 μm [8] with **1–4** for 2 hr. Centrifugation, extensive washing of the precipitated metal with buffer, treatment with β-mercaptoethanol to detach any adsorbed virus or protein, and analysis by

[3]Correspondence: jackj@scripps.edu (J.E.J.)
mgfinn@scripps.edu (M.G.F.)

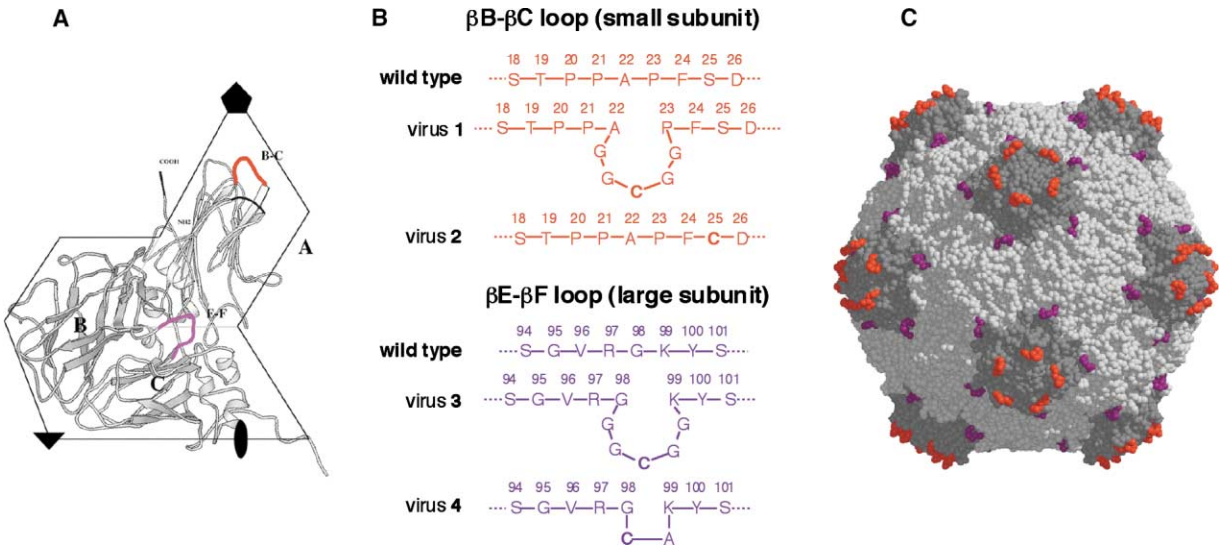

Figure 1. Cysteine-Added Mutants of CPMV

(A) The atomic structure of the CPMV coat protein, with the sites of mutational insertion highlighted in red (βB-βC loop) and purple (βE-βF loop).

(B) Amino acid sequences corresponding to native and mutant CPMVs **1–4**.

(C) A model structure of the entire particle shows the addition of a 5 residue insert (GGCGG) at the two positions of interest in the wild-type CPMV structure. The resulting mutant viruses correspond to **1** and **3**. Note that the BC loop resides farther "up" on the protruding cap than the EF loop at each 5-fold axis of the icosahedral structure.

denaturing gel electrophoresis and RT-PCR gave the results shown in Figure 2. Very little viral protein from wild-type CPMV was shown to be coprecipitated with gold, demonstrating that CPMV remains intact and does not possess exposed cysteine residues that bind to the metal surface (denatured wild-type protein was independently shown to bind to the metal particles). In contrast, the Cys mutants all showed substantial adsorption, indicated by analysis of both viral protein (Figure 2A) and viral RNA by RT-PCR (Figure 2B). When the gold particles were pretreated with BME, DTT, or TCEP, washed, and then exposed to the cysteine mutants, no binding was observed (data not shown). In addition, the interaction of thiol-derivatized viruses with gold was visualized directly by TEM (Figure 2C). Bulk aggregation was observed when freshly prepared gold particles were mixed with any of the cysteine mutants, but not when they were mixed with wild-type CPMV, the result of the polyvalent display of thiols around the mutant capsid structures. Isolated gold particles in such samples showed adhered viruses when they were stained and examined at sufficient magnification. The binding of 5 nm colloidal gold particles was also observed by TEM and will be fully described elsewhere.

Organic Reactivity

The thiol groups of the introduced Cys residues of the mutant viruses **1–4** are active nucleophiles toward maleimide and haloacetamide electrophiles. Thus, the selective reactivities of the three more stable viruses **2–4** were demonstrated by titration with fluorescein maleimide **5** in a buffer-DMSO mixture (equation 1 in Figure 3). All three viruses behaved similarly in that they showed complete reaction at pH 6 within 6 hr at 4°C and thereby demonstrated much higher reactivity than the wild-type virus (Figure 4). Highlighting the different sites of attachment, SDS-PAGE of the resulting viral proteins showed dye attachment to the small subunit for **2** and to the large subunit for **3** (Figure 4). The S-alkylated viruses did not aggregate in the absence of added reducing agents and did not bind to metallic gold. The particles remained intact, as shown by electron microscopy, sucrose gradient centrifugation, and size-exclusion chromatography. Fluorescein-modified particles were easily separated from nonmodified viruses by ion-exchange FPLC (Figure 4).

We have previously described the selective attachment of monomaleimido-Nanogold to the thiol residues of **3** (equation 2 in Figure 3), as well as the cryo-electron microscopy imaging of the resulting construct [1]. Nanogold attachment can also be revealed by silver enhancement, as shown in Figure 5. Thus, analogous to treatment of the virus with uranyl acetate (Figure 5C), addition of silver-staining solution [9, 10] to wild-type CPMV gave only a limited amount of negative staining. In contrast, the attached Nanogold clusters nucleated the efficient deposition of silver, providing a positive stain of the virus particles (Figure 5D).

Controlled Aggregation

The commercially available biocytin reagent **6** was used to decorate the surface of CPMV mutants **2** and **3** with biotin groups (equation 3 in Figure 3). The employed reaction condition reproducibly gave the attachment of 20 ± 2 dye-maleimide molecules (equation 1 in Figure 3), and so we assume that the biotin loading was similar. The biotinylated particles, but not wild-type CPMV, were each shown to bind tightly to columns bearing immobi-

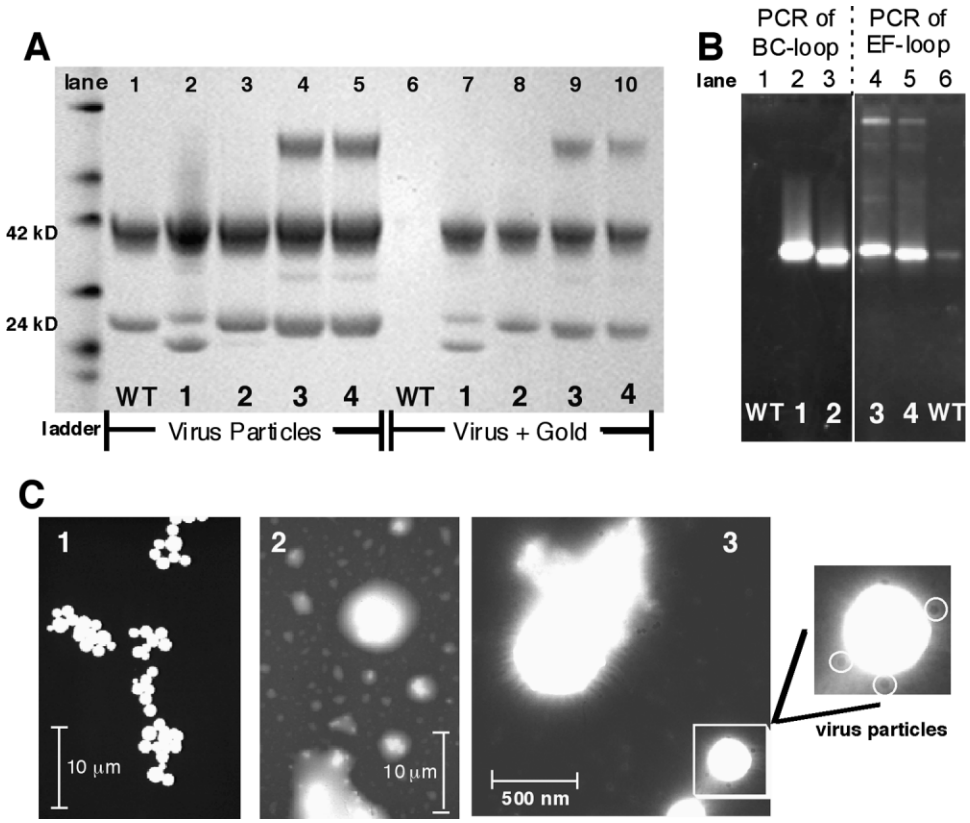

Figure 2. Evidence for the Binding of Cysteine Mutants to Metallic Gold

(A) SDS-PAGE analysis of wild-type and mutant CPMV viruses **1–4** (lanes 1–5) and analogous samples isolated from coprecipitation with metallic-gold particles (lanes 6–10; see text). The 42 kDa AND 24 kDa bands are the large and small subunits of CPMV, respectively. The high molecular-weight band above the main band in lanes 4, 5, 9, and 10 has been tentatively assigned to an aggregate involving the small subunit of **3** or **4**. Lanes 2 and 7 show that the small subunit of **1** undergoes substantial cleavage, presumably at the inserted loop.

(B) RT-PCR analysis of the genetic material isolated from coprecipitation of the following viruses with gold particles: lanes 1 and 6, WT-CPMV; and lanes 2–5, mutants **1–4**. PCR was done only on the sections encompassing the BC loop (237 base pairs) and the EF loop (147 base pairs), as indicated. Note that the appearance of a faint band in lane 6 shows a very small amount of nonspecific adsorption by the wild-type virus to gold.

(C) TEM images of gold particles and virus **1**. (1) freshly prepared Au particles with an average diameter of 0.9 μm (unstained). (2) Au particles treated with a 0.3 mg/ml solution of virus **1** for 12 hr (unstained). (3) A different position on the grid of sample 2, after staining with uranyl acetate. Virus particles (appearing dark by virtue of the negative stain) can be seen surrounding each of the bright Au clusters; on the right is a magnified view of a single Au particle surrounded by several viruses, some of which are circled in white.

lized avidin. Adding soluble avidin to these virions was expected to give crosslinked networks because there are four biotin binding sites per tetrameric avidin molecule. As shown in Figure 6, the formation and appearance of the resulting gels depends upon the location of the inserted cysteine residues and the concentration of the virus. Thus, mixing **2**-$(biotin)_{20}$ with avidin caused the immediate formation of a white precipitate, even when the component solutions were quite dilute (<1 mg/ml virus). A representative TEM image could not be obtained because of the extensive crosslinking of such samples. In contrast, biotinylated **3** and avidin formed neither a precipitate nor a visible gel at virus concentrations as high as 15 mg/ml, but aggregation did occur, as shown by TEM (Figure 6B). Under more dilute conditions, discrete two-dimensional arrays of particles were generated (Figure 6C). No evidence of aggregation by any assay was evident in the absence of avidin or when undecorated virus particles were used instead of the biotinylated ones.

Addressing of Multiple Reactive Sites

Except for the added residues, the cysteine mutants of CPMV possess the same structure as the wild-type virus, and they were therefore expected to retain their natural chemical reactivity in addition to that of the inserted thiols. In particular, the small subunit's uniquely reactive Lys38, described in the preceeding paper, was independently derivatized by amine-selective reagents. Thus, separate samples of virus **3** were loaded with 60 fluorescein molecules on the external thiols (as per equation 1 in Figure 3; also Figure 4) and 60 fluoresceins on the external lysines (Figure 7). Each of the resulting purified adducts was then treated with the complementary functionalized dye to alkylate the remaining type of nucleophilic residue. Figure 7 shows uv-vis spectra and SDS-PAGE analysis of a set of virus-dye conjugates from mutant **3**. Viruses **2** and **4** give very similar results, with the exception that the reactive exterior thiol residues of **2** are located on the small subunit.

We have previously observed that native CPMV con-

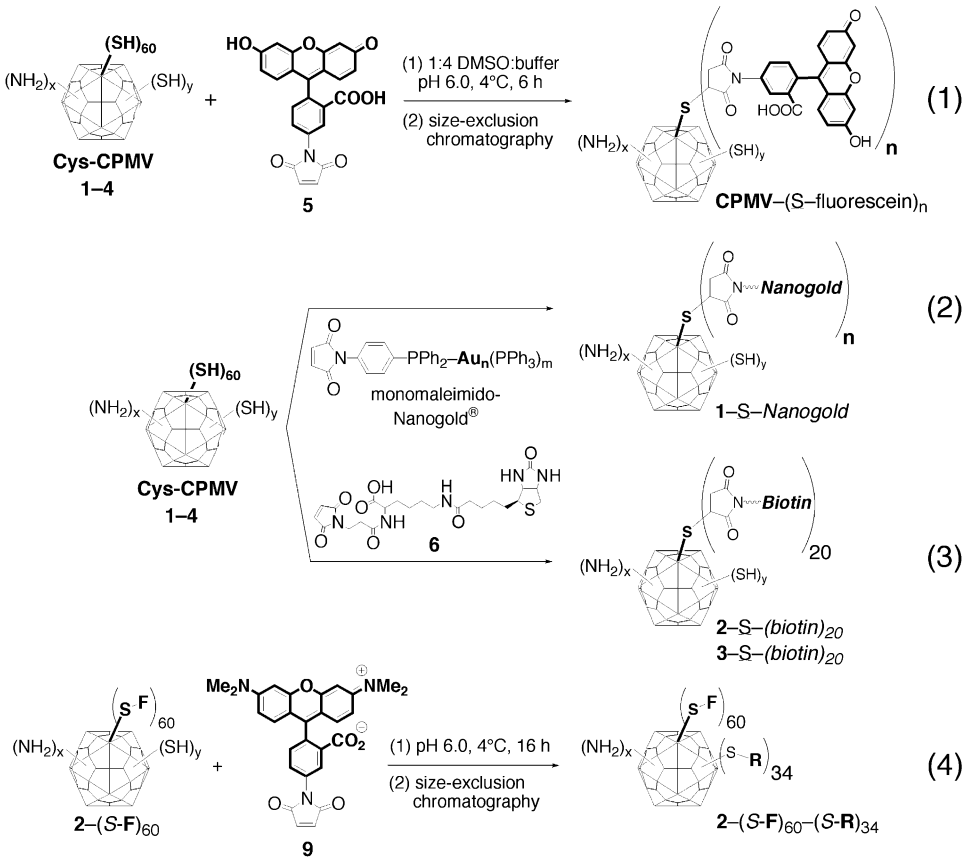

Figure 3. Attachment Reactions to Mutant CPMV Particles

tains two reactive cysteine residues on the *interior* surface of the capsid structure and that these react quite sluggishly compared to the exterior thiols of the mutant viruses [1]. It is therefore possible to address these two types of positions sequentially under controlled conditions. For example, a reaction of **2** with 50 equivalents (per protein asymmetric unit) of **5**, subsequent purification, then reaction with 500 equivalents of 5-maleimide tetramethylrhodamine (**9**) overnight at 4°C gave CPMV decorated with an average of 60 fluoresceins and 34 rhodamines per particle, as determined by uv-vis absorbance spectroscopy (equation 4 in Figure 3).

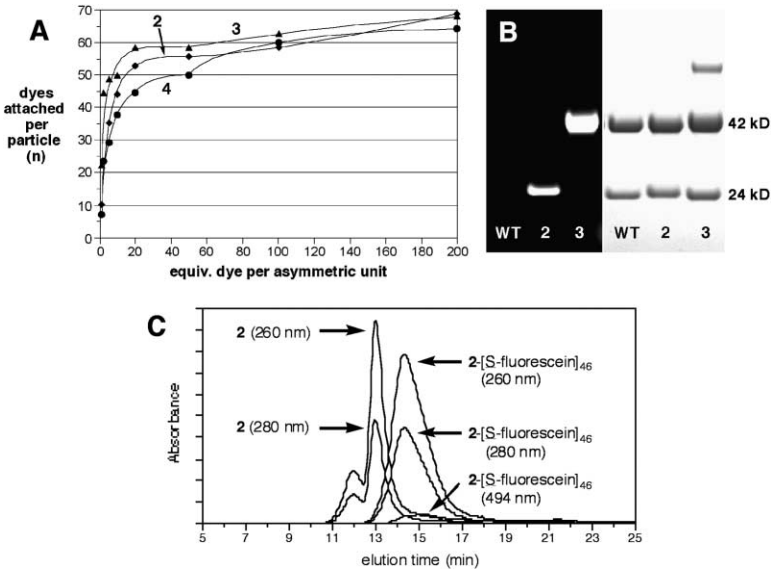

Figure 4. Attachment of Fluorescein to CPMV Mutants via Reagent **5**

See also equation 1 in Figure 3.

(A) Relationship of the amount of **5** used to the number of attached dyes per CPMV particle for the mutant viruses **2–4**. Note that there are 60 asymmetric units per virus particle. Each data point shown is the average of three independent experiments with a maximum error of ±10% of the reported attachment value.

(B) Denaturing protein gel showing specific labeling of small and large subunits for **2** and **3**, respectively. On the black background is shown the gel visualized directly under ultraviolet illumination, giving light bands at the sites of fluorescein attachment. On the white background is shown the result of standard staining with Coumassie blue to reveal both protein subunits.

(C) Anion-exchange FPLC of virus **2**, and **2** derivatized with fluorescein, under identical elution conditions. Retention times are highly reproducible, and mixtures of the viruses have been readily separated in this way.

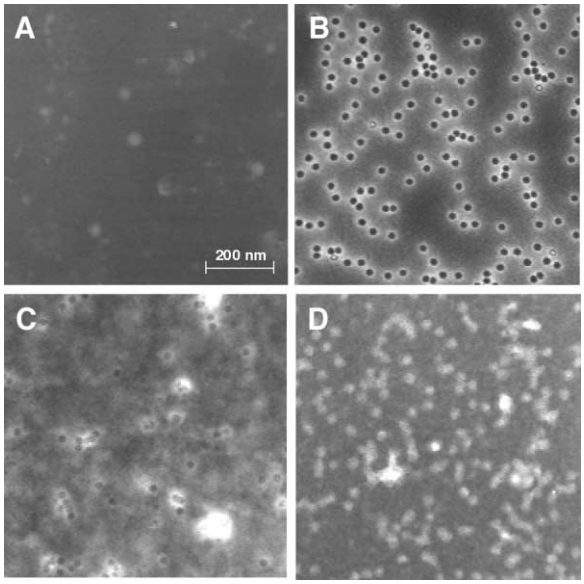

Figure 5. TEM of Nanogold-Decorated **1**

(A) **1**-S-Nanogold without staining.
(B) **1**-S-Nanogold stained with uranyl acetate.
(C) **1** treated with silver enhancement reagent.
(D) **1**-S-Nanogold with silver enhancement.

Significance

The cysteine mutants described here are emerging as the most versatile of virus-based starting materials for chemical synthesis because of their selective and potent reactivity, high expression yields, and exceptional stability. We have also demonstrated the controlled attachment of polymer chains, carbohydrate derivatives, oligonucleotides, and other small molecules to these templates, as will be described elsewhere. The most exciting applications will be those that take advantage of the polyvalency and self-assembling properties of such virus building blocks.

Experimental Procedures

General

Dye reagents **5–9** were purchased from Molecular Probes. Unless otherwise indicated, "buffer" refers to 0.1 M potassium phosphate (pH 7.0). Gold particles of average 0.9 μm diameter were prepared by the method of Goia and Matijevic [8]. Transmission electron microscopy, sucrose gradient ultracentrifugation, ion-exchange FPLC, and avidin column binding of biotinylated virus were performed as described in the accompanying paper. Modification of cysteine mutants with thiol-reactive dye reagents was performed as previously described [1], and the virus conjugates were characterized analogously to those described in the accompanying paper.

Preparation of Cysteine-Added Mutants of CPMV

Infectious clones pCP1 and pCP2, containing the full-length cDNA copies of CPMV RNA-1 and RNA-2 respectively, were constructed by Lomonossoff [11]. Plasmid pCP2 has been further modified as cloning vectors (pCP2-L1 and pLgEF). (For pCP2–L1, see [12]. Vector pLgEF was constructed based on pCP2, and details will be described elsewhere). Vector pCP2-L1 was used for construction of chimeric plasmids pBCCysα (for mutant virus **1**) and pBCCysγ (for mutant virus **2**). Vector pLgEF was used for construction of chimeric plasmids pEFCysα and pEFCysβ (for viruses **3** and **4**, respectively). Bacterial plasmids were propagated in *E. coli* strain XL-1 Blue (Stratagene) and DH5α. The propagation and purification of the viruses were performed by standard methods [13].

Binding with Metallic Gold

Virus (0.2 mg) and freshly prepared 0.9 μm-diameter gold (7 mg) were mixed together in buffer (100 μl). After gentle agitation for 2 hr at 4°C, the mixture was centrifuged at 16,000 *g* for 2 min. The supernatant was carefully removed, and the pellet was washed with 0.1 M potassium phosphate (pH 7.0) buffer (6 × 500 μl), PBS buffer with 0.1% Tween-20 (3 × 500 μl), and 0.1 M potassium phosphate (pH 7.0) buffer again (2 × 500 μl), each time with full resuspension and then centrifugation of the pelleted material. The final pellet was used for protein and RT-PCR analysis (Figure 2), as follows.

For protein analysis by polyacrylamide gel electrophoresis, 3 mg of pelleted material was resuspended in a mixture of water (12 μl) and β-mercaptoethanol (3 μl), then mixed with NuPage loading buffer (5 μl). The mixture was heated at 95°C for 5 min, loaded on NuPage 4%–12% Bis-Tris precast gel, and run at 100 V for 2 hr. For RNA analysis, the pellet (1 mg) was resuspended in 100 μl RNA extraction buffer, containing 100 mM glycine, 10 mM EDTA, 0.1 M NaCl, and 2.5 mg/ml bentonite (pH 9.5). Phenol/chloroform extraction and ethanol precipitation followed. For samples derived from **1** and **2**, the resulting RNA was annealed to primer pBCCC2 (ATA-

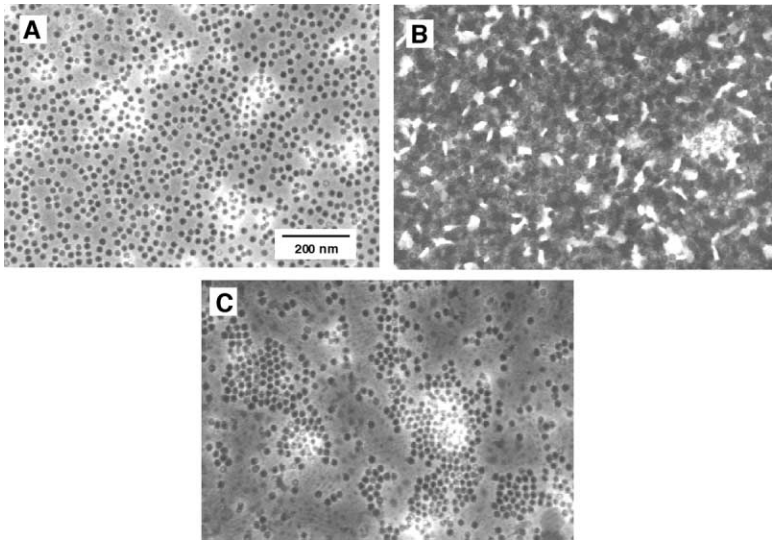

Figure 6. Negative-Stain Electron Microscopy Images of Aggregation of Virus-Biotin Conjugates with Avidin.

(A) **2**-$(biotin)_{20}$ (0.1 mg/ml).
(B) **3**-$(biotin)_{20}$ (15 mg/ml) plus avidin (2.5 mg/ml); the mixture was diluted by a factor of 100 before TEM observation.
(C) **3**-$(biotin)_{20}$ (1.5 mg/ml) plus avidin (0.5 mg/ml); the mixture was diluted by a factor of 10 before TEM observation. Note the regions showing organized two-dimensional arrays of particles.

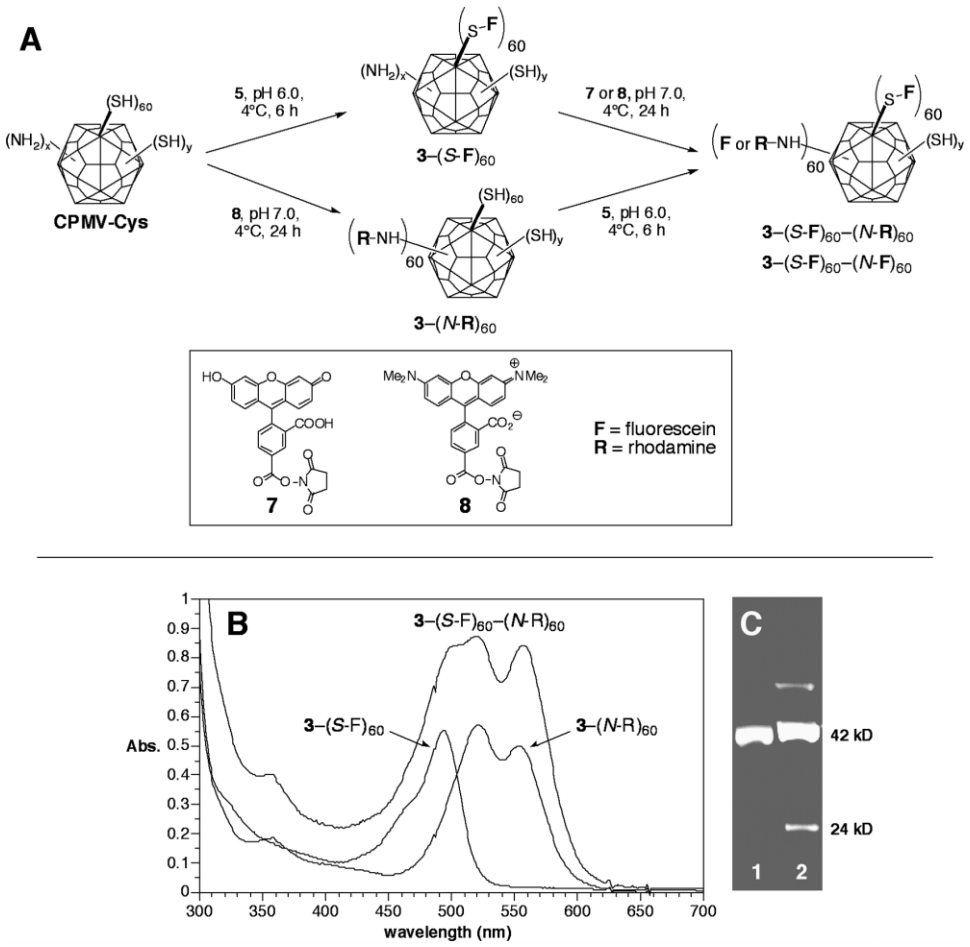

Figure 7. Site-Specific Double Labeling of Mutant CPMV **3**

(A) Synthetic routes; each dye attachment was followed by purification by size-exclusion chromatography.

(B) The uv-vis absorbance spectra of the indicated virus-dye conjugates.

(C) Denaturing protein gel showing specific labeling of small and large subunits, visualized directly under ultraviolet illumination: lane **1**, **3**–(S-F)$_{60}$; lane 2, **3**-(S-F)$_{60}$-(N-F)$_{60}$.

GTT-CCA-GAT-TTC-CA, which binds to nucleotides 2852–2868 of RNA-2 of CPMV, for the analysis the βB-βC loop of the small capsid protein); for samples derived from **3** and **4**, pLGEF2 (CTA-ACT-CTG-CTT-CGA-CT, which binds to nucleotides 1961–1977 of RNA-2 of CPMV, for the analysis the βE-βF loop of the big capsid protein) was used. The first strand of cDNA was synthesized with M-MLV reverse transcriptase, followed by PCR analysis with primers pBCCC1 (TCC-CGC-TTG-CTT-GGA-GC) and pBCCC2 for **1** and **2** and pLGEF1 (CGC-ACC-CAT-GTT-ATA-AC) and pLGEF2 for **3** and **4**.

For TEM analysis of gold-virus mixtures (Figure 2), virus (0.5 mg) and 0.9 μm gold (2 mg) were mixed together in 500 μl buffer. After gentle agitation for 30 min at 4°C, 20 μl of the mixture was used for preparation of the EM grid.

Modification of Viruses with Nanogold Reagent and Biotin

Monomaleimido Nanogold (6 nmol) was dissolved in isopropanol (20 μl), then mixed with **1** (0.1 mg) in 200 μl buffer. After incubation at 4°C for 12 hr, the mixture was purified by size-exclusion chromatography. The product was analyzed with TEM directly, with uranyl acetate staining, and with HQ silver enhancement reagent [14], as indicated in Figure 5. Biotinylation of cysteine mutant viruses was accomplished by the general derivatization procedure with viruses **2** and **3** and the reagent 3-(N-maleimidylpropionyl)biocytin (50-fold molar excess with respect to the concentration of viral protein).

Acknowledgments

We thank The Skaggs Institute for Chemical Biology (Q.W. is a Skaggs Postdoctoral Fellow), The David and Lucille Packard Foundation Interdisciplinary Science Program, and the Naval Research Laboratory (N00014-00-1-0671) for support of this work. We are grateful to Dr. G. Lomonossoff for a gift of the infectious CPMV clones pCP1, pCP2, and derivatives.

Received: March 20, 2002
Revised: May 23, 2002
Accepted: May 23, 2002

References

1. Wang, Q., Lin, T., Tang, L., Johnson, J.E., and Finn, M.G. (2002). Icosahedral virus particles as addressable nanoscale building blocks. Angew. Chem. Int. Ed. *41*, 459–462.
2. Porta, C., Spall, V.E., Lin, T., Johnson, J.E., and Lomonossoff, G.P. (1996). The development of Cowpea mosaic virus as a potential source of novel vaccines. Intervirology *39*, 79–84.
3. Fernández-Fernández, M.R., Martínez-Torrecuadrada, J.L., Casal, J.I., and Garcia, J.A. (1998). Development of an antigen

presentation system based on plum pox potyvirus. FEBS Lett. *427*, 229–235.

4. Lomonossoff, G.P., and Hamilton, W.D.O. (1999). Cowpea mosaic virus-based vaccines. Curr. Top. Microbiol. Immunol. *240*, 177–189.
5. Taylor, K.M., Lin, T., Porta, C., Mosser, A., Giesing, H., Lomonossoff, G.P., and Johnson, J.E. (2000). Influence of 3-dimensional structure on the immunogenicity of a peptide expressed on the surface of a plant virus. J. Mol. Recognit. *13*, 71–82.
6. Lin, T., Porta, C., Lomonossoff, G., and Johnson, J.E. (1996). Structure-based design of peptide presentation on a viral surface: the crystal structure of a plant/animal virus chimera at 2.8 Å resolution. Fold. Des. *1*, 179–187.
7. McLain, L., Porta, C., Lomonossoff, G., Durrain, Z., and Dimmock, N.J. (1995). Human immunodeficiency virus type 1 neutralizing antibodies raised to a lipoprotein 41 peptide expressed on the surface of a plant virus. AIDS Res. Hum. Retroviruses *11*, 327–334.
8. Goia, D.V., and Matijevic, E. (1999). Tailoring the particle size of monodispersed colloidal gold. Coll. Surf. A Physiochem. Eng. Asp. *146*, 139–152.
9. Hainfeld, J.F., and Furuya, F.R. (1995). Silver enhancement of Nanogold and Undecagold. In Immunogold-Silver Staining: Principles, Methods and Applications, M.A. Hayat, ed. (Boca Raton, FL: CRC Press), pp. 71–96.
10. Humbel, B.M., Sibon, O.C.M., Stierhof, Y.-D., and Schwarz, H. (1995). Ultra-small gold particles and silver enhancement as a detection system in immunolabeling and in situ hybridization experiments. J. Histochem. Cytochem. *43*, 735–737.
11. Dessens, J.T., and Lomonossoff, G.P. (1993). Cauliflower mosaic virus 35S promoter-controlled DNA copies of Cowpea mosaic virus RNAs are infectious on plants. J. Gen. Virol. *74*, 889–892.
12. Dalsgaard, K., Uttenthal, X., Jones, T.D., Xu, F., Merryweather, A., Hamilton, W.D.O., Langeveld, J.P.M., Boshuizen, R.S., Kamstrup, S., Lomonossoff, G.P., et al. (1997). Plant-derived vaccine protects target animals against a virus disease. Nat. Biotechnol. *15*, 248–252.
13. Siler, D.J., Babcock, J., and Bruening, G. (1976). Electrophoretic mobility and enhanced infectivity of a mutant of Cowpea mosaic virus. Virology *71*, 560–567.
14. Nanoprobes, Inc., www.nanoprobes.com.